Histol Histopathol (2026) 41: 553-566

Histology and Histopathology
From Cell Biology to Tissue Engineering

REVIEW Open Access

Microscopic studies on the structure of microornamentation and adhesive setae in normal and regenerating tail scales of some geckos

Antonio Bonfitto[1] and Lorenzo Alibardi[1,2]

[1]Department of Bigea, University of Bologna, Bologna and [2]Comparative Histolab, Padova, Italy

Summary. The present review summarizes recent information on the formation and fine structure of epidermal microornamentation and adhesive setae in scale pads of the tail in some arboreal geckos. The study utilizes transmission and scanning electron microscopy, in conjunction with immunolabeling, to detect the main proteins of the microornamentation, known as Corneous Beta Proteins. These are special small proteins with a central region containing beta-sheets that form most of the corneous material of scales and pads. These proteins are packed into long cords that form short spinulae or longer setae. In tail scales, the spinulae feature different shapes but possess a limited size, 0.5-2.0 µm. In sparse areas located toward the distal part of the tail, some scales form adhesive pads, and their microornamentation grows longer, forming setae of 10-30 µm in length in the species studied herein. This process gives rise to stiff but flexible bristles that arboreal geckos use for adhesion on vertical or inverted substrates or tree branches. During tail regeneration, some scales also regenerate the adhesive setae and give rise to new adhesive pads. Caudal setae are formed by a process similar to that observed during the formation of digital setae. This derives from the interaction of a specific epidermal layer (clear) with another layer (Oberhäutchen), which are formed in the scale pads. Setae vary in length, diameter, or terminal arborization, and they resemble those of the digits, albeit shorter. The presence of caudal adhesive pads reinforces the prehensibility and maneuverability of these arboreal lizards in their environment.

Key words: Gecko lizards, Scales, Microornamentation, TEM, SEM, Immunolabeling

Corresponding Author: Lorenzo Alibardi, Department of Bigea, University of Bologna, Bologna, Italy. e-mail: lorenzo.alibardi@unibo.it
www.hh.um.es. DOI: 10.14670/HH-18-983

The scale surface in geckos forms variable microornamentation

The epidermal surface of the scales in numerous lizards of the family Gekkonidae is sculptured in a typical pattern of microornamentation known as "spinulated" (Ruibal, 1968; Maderson, 1970; Hiller, 1972; Irish et al., 1988; Bauer, 2019; Riedel et al., 2019). These microstructures derive from the differentiation of the superficial epidermal layer, known as Oberhäutchen of the gecko epidermis, interfaced with another layer, the clear layer (Maderson et al., 1998; Alibardi, 1999, 2018). The functions of microornamentation can be multiple, from coordinating skin shedding, light scattering influencing animal visibility, dust or parasite cleaning, microorganism defense, humidity collection, etc. (Maderson et al., 1998; Arnold, 2002; Riedel et al., 2019; Riedel and Schwarzkopf, 2022). Spinulae possess nanoscale dimensions, 0.2-1.5 µm, and derive from different processes of accumulation of corneous material on the surface of Oberhäutchen cells. These processes give rise to a number of microstructure variations; however, three main patterns have been described in geckos in addition to the prevalent spinulated pattern, known as "corneous belts", "dendritic ramification", and "serpentine pit and groove" patterns (Bonfitto et al., 2022, 2023a,b).

Numerous geckos, in the terminal parts of their digits, possess rows of modified scales known as pad lamellae, where the spinulae of their outer surface undergo a process of extensive elongation giving rise to bristles of 10-100 µm in length, known as setae (Maderson, 1970; Hiller, 1972, 1975; Alibardi, 1999, 2018; Gamble et al., 2012; Bauer, 2019; Russel et al., 2019; Russell and Garner, 2021; Griffing et al., 2022; McCann and Hagey, 2024). The association of more lamellae in localized areas of the tail (or digits) forms a pad of lamellae or scansor. The formation of thousands to millions of setae on the surface of the pad lamellae determines the formation of a soft and sticky surface in these modified digital scales that can strongly adhere to

almost any type of natural or artificial substrate (Niewiarowski et al., 2016; Bauer, 2019; Russell et al., 2019). The terminal part of the setae branches differently in various species, and each branch terminates with the region of contact with the substrate, known as the spatula, with dimensions in the range of 50-200 nm. From the size of the spines to that of really adhesive setae, a range of spinulated elongations has been described, such as spine, spike, prong, setae-prong, and finally setae, the latter intensely involved in adhesion (Russell and Garner, 2021). Digital pads allow these geckos to climb vertical and inverted surfaces, and numerous of these lizards have an arboreal lifestyle (Gamble et al., 2012; Collins et al., 2015; Bauer, 2019; Russell and Gamble, 2019; Griffing et al., 2022; McCann and Hagey, 2024).

Microscopic, ultrastructural, and immunolabeling studies have shown that the clear layer of digital pads likely molds the growing spinulae formed in the contacting Oberhäutchen cells, allowing the formation of the setae. Although the mechanism is not yet known, it is the cytoskeleton present in the cytoplasm of clear cells that is involved in the formation of the setae (Hiller, 1972; Alibardi, 1999, 2020a,b, 2023; Kasper et al., 2024). Actin, tubulin, and RhoV, a small GTPase that modifies the actin meshwork and cell shape, are present in the growing setae of some geckos (*Tarentola mauritanica*, *Hemidactylus turcicus*, and *Phelsuma dubia*) and anoline lizards (*Anolis carolinensis* and *A. lineatopus*). Tubulin is also present in the growing setae cytoplasm of clear cells that surrounds the sete, forming spiral-shaped rings around the elongating setae. Plakophilin joins through numerous desmosomes in the plasma membrane of clear and Oberhäutchen cells during setae growth (Alibardi, 2020a). In the digital pads of the gecko *Chondrodactylus bibronii*, in addition to actin and tubulin, beta-catenin and desmoplakin are immunolocalized in punctuated adhesion junctions and desmosomes linking the membranes of clear cells that envelop the growing setae, supporting the molding action of the clear layer on setae formation from the Oberhäutchen layer (Kasper et al., 2024).

Adhesive pads are also found in the tails of some geckos

Although adhesive pads have been known and studied for many years in the digits of numerous species of geckos (Gamble et al., 2012; Russell and Gamble, 2019; Griffing et al., 2022), systematic reports on numerous species of geckos have also revealed the formation of pad lamellae in the tail also (Bauer, 1998). The main gecko families featuring tail pads include Phyllodactiline and Gekkonine from Africa, Australia, New Zealand and some Oceania regions, and New Caledonia. These species include mostly arboreal geckos, among which the genera *Hoplodactylus*, *Bavaya*, *Lygodactylus*, *Rachodactylus*, *Matoatoa*, *Urocotyledon*, and *Pseudothecadactylus* (Bauer, 1998; Griffing et al., 2021). These lizards utilize their functional and curled tail to help them move across the canopy where they live, with reinforced adhesion to the asperities of the branches. Some studies have shown that pads can also reform after loss and regeneration of the tail and its scales (Maderson, 1971; Alibardi and Meyer-Rochow, 2017; Alibardi and Bonfitto, 2019).

In this Review, we briefly summarize the current information on the morphology and formation of tail adhesive pads present in four species previously studied using light immunohistochemistry and transmission electron microscopy (TEM): the New Zealand common speckled gecko, *Hoplodactylus maculatus* (Diplodactylidae, now *Woodworthia maculata*; Alibardi and Meyer-Rochow, 2017); the New Caledonia crested gecko, *Rachodactylus ciliatus* (Diplodactylidae, now *Correlophus ciliatus*); the African Cape common dwarf gecko, *Lygodactylus capensis* (Gekkonidae); and the Cameroon dwarf gecko *Lygodactylus conraui* (Gekkonidae; Alibardi and Bonfitto, 2019; Bonfitto et al., 2022). The two species of *Lygodactylus* were those more extensively analyzed, in particular using the Scanning Electron Microscope (SEM) for the observation of the shape and distribution of their microornamentation.

LM-TEM of adhesive setae in the tail of *W. maculata* and *C. ciliatus*

No SEM observations were conducted on *W. maculata* and *C. ciliatus*, but the present observation can be integrated by consulting a SEM study on the skin of these species (Bauer, 1998; Griffing et al., 2021). The formation of new scales and pads in the tail of *W. maculata* derives from the initial downward growth of the multilayered wound (regenerating) epidermis of the regenerating tail that initiates at about one mm from the tip of the elongating tail in this species (Alibardi and Meyer-Rochow, 2017). The epidermis forms symmetric pegs (arrow in Fig. 1A) that become asymmetric in more advanced stages of regeneration, and internally begin to differentiate a layer of fusiform cells that will become the new corneous layers of the scales, the clear and Oberhäutchen layers first, followed by the beta-layer underneath them (Fig. 1B-D). In the regenerating pads, both clear and contacting Oberhäutchen cells become hypertrophic, while the following 3-5 layers of beta-cells appear as fusiform and more basophilic (darker after staining with toluidine blue; Fig. 1C,D). The following differentiation and cornification of the Oberhäutchen and beta-cells produces a thinner corneous layer while the clear layer is shed, revealing formed setae of 5-15 μm in length (Fig. 1E,F). Under TEM, the cytoplasm of the clear layer disintegrates among the setae of the Oberhäutchen, leaving free setae of 0.3-0.6 x 5-10 μm on the free surface of the pads (Fig. 1G).

The length of setae in the normal tail of *C. ciliatus* depends on the localization of pads along the tail, being more developed in the distal (caudal) region, by the tail

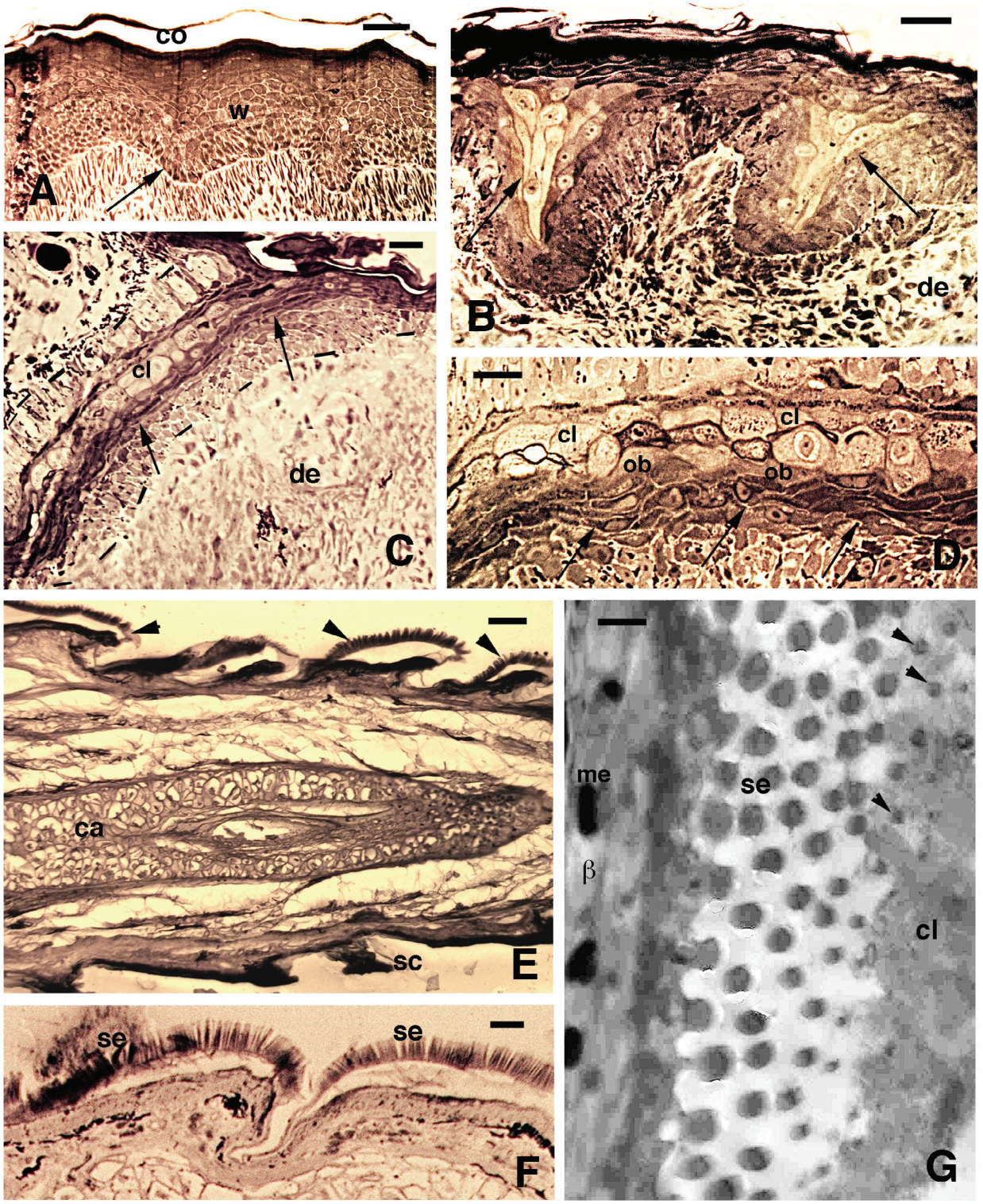

Fig. 1. Histology of regenerating scales in *W. maculata* (**A-F**, toluidine blue stain) and TEM detail on regenerated setae **(G)**. **A.** Apical waved epidermis with symmetric pegs (arrow). **B.** Asymmetric pegs with elongated differentiating central cells (arrows). **C.** Elongated epidermal peg (outlined by dashes), whose central region forms the darker beta-layer (arrows). **D.** Close-up on the forming shedding complex with granulated pale cells in contact with Oberhäutchen cells. Arrows indicate the underlying beta-cell layers. **E.** Longitudinal section of the terminal regenerated tail with the setae (arrowheads) of the pad lamellae indicated. **F.** Close-up of two pad lamellae. **G.** TEM view of formed setae cut transversally, with the distal sections included (arrowheads) in the degenerating cytoplasm of a clear cell. ß, beta layer; ca, regenerated cartilaginous cylinder; cl, clear (granulated) layer; co, corneous layer; de, dermis; me, melanosome; ob, Oberhäutchen; sc, tail scales; se, setae; w, wound epidermis. Scale bars: A, E, 20 μm; B-D, F, 10 μm; G, 0.5 μm.

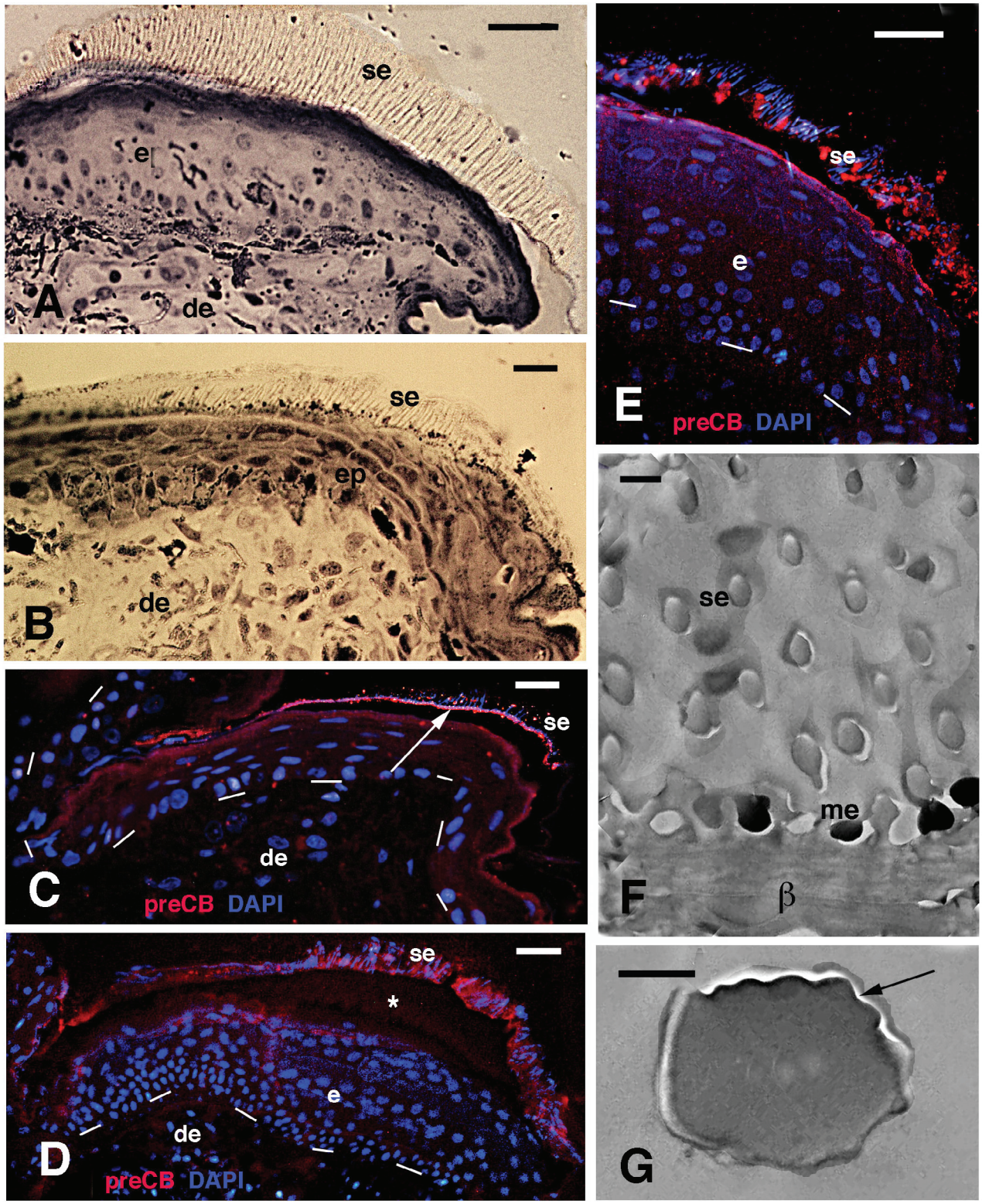

Fig. 2. Histology of normal tail scales in *C. ciliatus* **A, B.** Immunofluorescence using the pre-Core Box antibody for CBPs (C-E), and TEM images of the setae **(F, G)**. **A.** Pad lamella with thin setae. **B.** Other scale area showing shorter, thin setae. **C.** Immunolabeled beta-layer (arrow) sustaining very short setae. **D.** Pad lamella cut tangentially with a labeled beta-layer bearing short setae. The asterisk indicates artifact detachment of the setae from the epidermis. **E.** Close-up of short setae only partially immunolabeled. **F.** Fine electron microscopic detail of thin setae merged with the beta-layer. **G.** Magnification of a cross-sectioned seta featuring the irregular perimeter (arrow). ß, beta-layer; de, dermis; e, epidermis; me, melanosome; se, sete; w, wound epidermis. Dashes underline the epidermis. Scale bars: A, 20 μm; B-E, 10 μm; F, 0.5 μm; G, 0.25 μm.

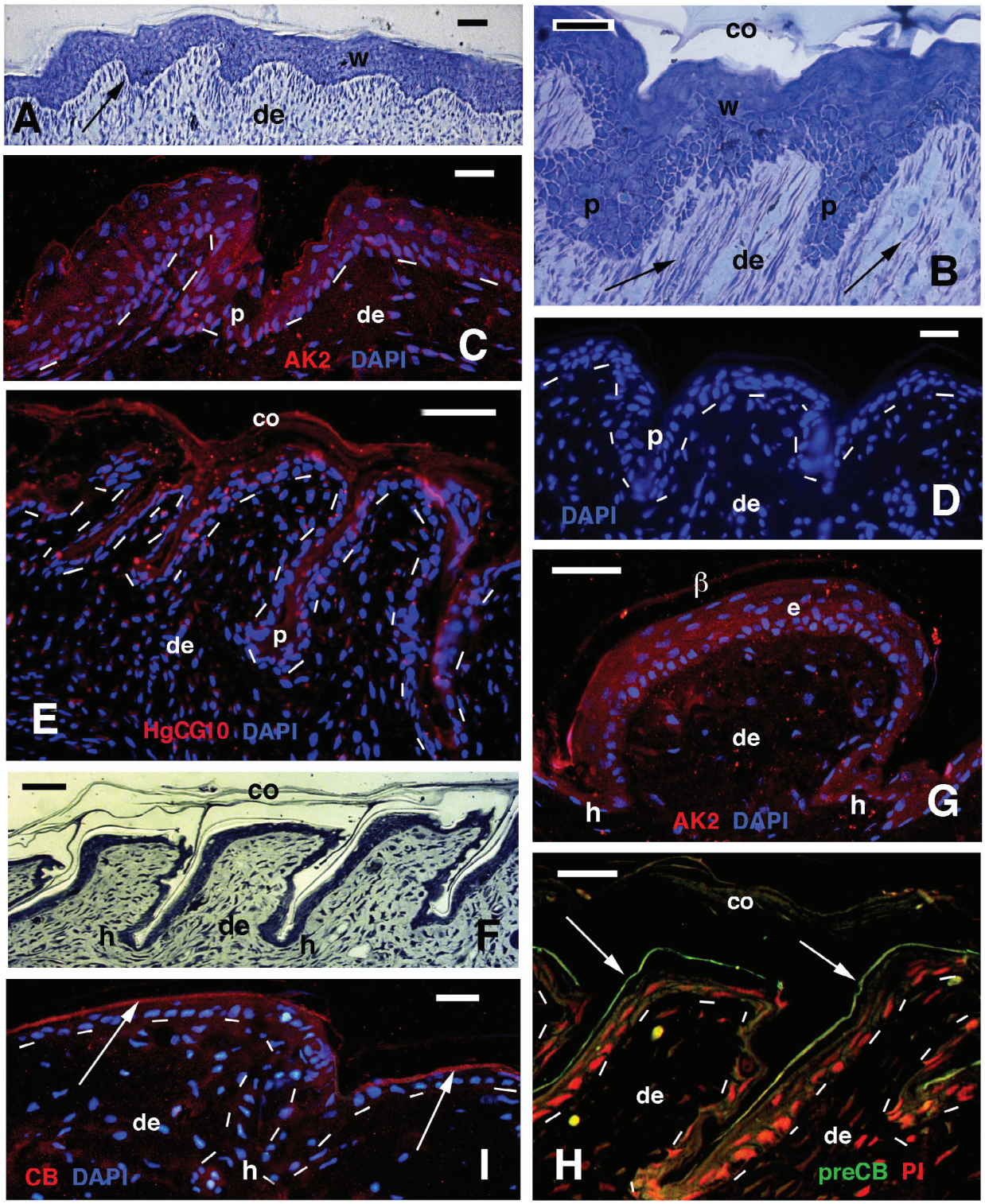

Fig. 3. Histology **(A, B, F)** and immunofluorescence **(C-E, G-I)** of regenerating scales in *L. capensis*. **A.** Waved apical wound epidermis. Toluidine blue stain. **B.** Formation of asymmetric pegs (arrows point to "stretched" fibroblasts). Toluidine blue stain. **C.** AK2-immunolabeled wound epidermis with peg. **D.** Epidermal outline of regenerating scales. **E.** Elongated narrow pegs showing weak immunolabeling for HgGC10 antibody for CBPs. **F.** After maturation of the corneous wound epidermis, it detaches from the underlying epidermis, revealing the new regenerated scales. Toluidine blue stain. **G.** Neogenic scale with AK2-immunolabeled epidermis. **H.** Neogenic scales with a thin immunolabeled (arrows) beta-layer. **I.** Other neogenic scales in resting condition (monolayer epidermis with few suprabasal cells) and a thin beta-layer (arrows). co, corneous layer of the wound epidermis; de, dermis; e, epidermis; h, hinge region (inter-scale); p, epidermal pegs; w, wound epidermis. Dashes underline the epidermis. Scale bars: A, B, E-H, 20 μm; C, D, I, 10 μm.

tip. In contrast, they disappear in more proximal areas (rostral) of the tail (Griffing et al., 2021). In our sections, the pad lamellae present in the distal part of the normal tail of *C. ciliatus* present numerous setae that measure 0.3-0.5 x 5-25 μm, depending on their position along the outer (dorsal) scale surface. The longer setae are positioned from about mid-length of the outer pad surface and become shorter and almost disappear in the proximal direction, toward the hinge region (Fig. 2A,B). The setae react weakly and unevenly to pre-core box antibody (against a specific region of lizards' Corneous Beta Proteins, see Alibardi, 2018, 2020a,b), while immunofluorescence is higher in the narrow beta-layer located at the base of setae and lowers to disappear in the differentiating layers located underneath (Fig. 2C-E). No other tissues, epidermis or dermis, react with this antibody. Under TEM, the setae appear quite thin, about 0-4-0.5 μm in diameter at their base, which is merged with the electron-pale beta-layer, and thin out at their apex (Fig. 2F). In cross-section, setae show an oval to a roundish shape, and their surface appears undulated or even denticulated (Fig. 2G).

LM-TEM study on adhesive setae in the tail of *Lygodactylus capensis* and *L. conraui*

In the two species of *Lygodactylus* analyzed herein, the cytological characteristics of the setae appear similar. In *L. capensis*, their formation and structure have been analyzed in the regenerating tail (Alibardi and Bonfitto, 2019). The waved wound epidermis formed in distal areas of the regenerating tail produces symmetric epidermal pegs, which become asymmetric and deeper as they move toward proximal areas of the regenerating tail (Fig. 3A-E). Dermal fibroblasts appear perpendicularly oriented ("stretched") to the epidermal surface during the formation of these pegs, which become deeper in more proximal regions (Fig. 3A,B). As the pegs elongate into the dermis, the formation of new corneous layers of the beta-generation initiates in the central-axial region of the pegs, as also indicated from the weak immunolabeling for CBPs (such as that revealed by the HgCG10 antibody; Fig. 3E). Later, as the beta-layer matures in the center of the more proximal pegs, the latter split, giving rise to new or regenerated scales. Keratinocytes of the wound epidermis of the pegs and neogenic scales are immunolabeled with the AK2 antibody, directed to an acidic Intermediate Filament keratin (IF-keratin, Alibardi, 2014; Fig. 3C,G). The new scales (regenerated or neogenic) form a thin and compacted beta-layer underneath the corneous part of the wound epidermis that is later shed, revealing the new scales (Fig. 3F,H,I). The compact beta-layer is variably immunolabeled with different antibodies against CBPs (the core-box and pre-core box antibodies; see Alibardi, 2014, 2018, 2020a,b), however, not with the AK2 antibody for an acidic IF-keratin (Fig. 3H,I).

When a second cycle of shedding starts, the outer epidermal generation is composed of a thin external beta-layer, a largely immature alpha-layer, where numerous flat cells are still present, and underneath, a thin pale line indicates the formation of the inner Oberhäutchen (the pale line represents the initial formation of the spinule; Fig. 4A). CBP immunolabeling shows the immunolabeled and compact outer beta-layer and the inner beta-layer (forming), made of fusiform-shaped beta-cells (Fig. 4B). The formation of pads follows the general process described above, but in these scales, the spines elongate into setae. Random sectioning of the normal tail in *L. conraui* reveals that some scales, located more proximally in the tail, possess very short setae (arrow in Fig. 4C). Complete pads with longer setae, 10-25 μm in length, are formed by the distal areas of the regenerated tail or near the tail tip at 30-45 days of regeneration (Fig. 4D,E). Both the outer and especially the inner (forming) setae appear immunolabeled for CBPs, using core-box or pre-core-box antibodies (Fig. 4F,G).

After immunogold-labeling under TEM with CBP antibodies, the mature beta-layer is the more intensely labeled tissue, even more than the Oberhäutchen spinulae (Fig. 5A). During renewal of the epidermis, numerous inner setae are formed from Oberhäutchen cells (Fig. 5B) and give rise to the pale line observed under light microscopy (LM) (Figs. 4A, 5B). Small beta-packets accumulate in the cytoplasm of Oberhäutchen cells and are immunogold labeled for CBPs (double arrowhead in Fig. 5C). The labeling extends into the setae that are surrounded by an immuno-negative ring of denser fibrous material, representing the cytoskeleton of clear cells (arrows in Fig. 5C). Studies on other gecko species have indicated that actin and tubulin are part of this cytoskeleton (Alibardi, 2020a; Kasper et al., 2024). This immunolabeled material, made of cysteine-rich CBPs, progressively accumulates inside the growing setae (arrowheads in Fig. 5C; Alibardi, 2018, 2023). The immunolabeling of beta-packets is also observed in the cytoplasm of differentiating beta-cells that are forming underneath Oberhäutchen cells (Fig. 5D). After beta-cells are packed and fully differentiated, together with the merged basal part of the Oberhäutchen, they form the thin corneous lamina (beta-layer) sustaining the setae.

SEM of adhesive setae in the tail of *Lygodactylus capensis* and *L. conraui*

The microornamentation pattern in the two species is substantially similar. Tail scales, normal or regenerated in *Lygodactylus capensis*, and normal tail scales in *Lygodactylus conraui*, are covered by dense micro-ornamentation. This results from the presence of spinulated protrusions whose length varies from 0.5 to about 2 microns (Fig. 6 A,B). Small bare areas (naked Oberhäutchen) are occasionally detected, especially toward the tips of dorsal scales (arrows in Fig. 6A). At higher magnification, the thin lines observed on the surface generally delimit the polygonal shape of Oberhäutchen cells (arrows in Fig. 6B). The shape,

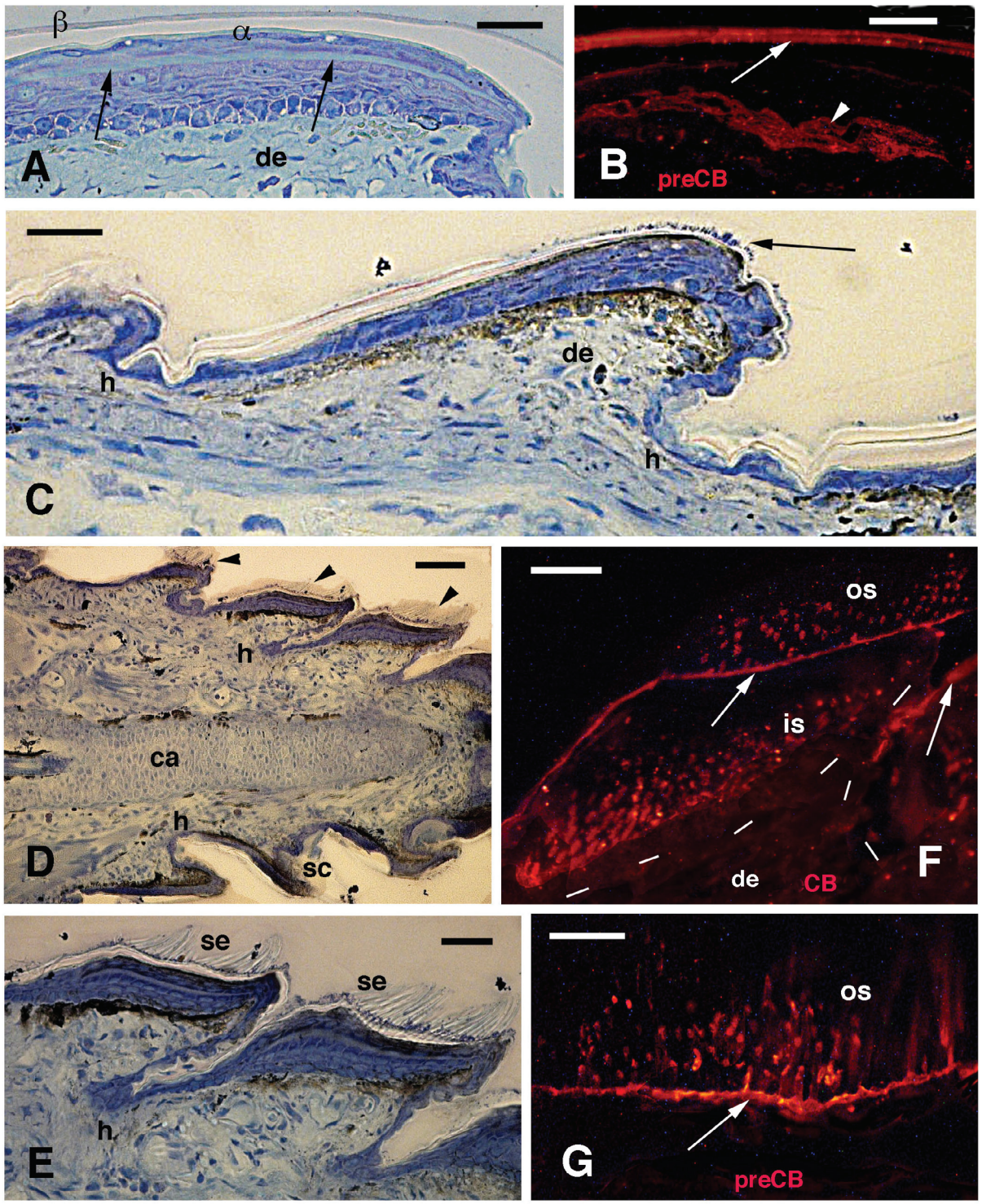

Fig. 4. Histology (**A, C-E**, toluidine blue stain) and immunofluorescence **(B, F, G)** of regenerating tail scales in *L. capensis*. **A.** Scale (likely a short pad lamella) showing a pale line (arrows) underneath the alpha-layers of the outer generation, indicating formation of the shedding layer (short setae). **B.** Detail showing the two generations of beta-cells immunofluorescent for the preCore Box antibody against CBPs. The arrow indicates the outer beta-layer, the arrowhead the inner (forming) beta-layer. **C.** A pad lamella with very short setae (arrow) is present among other tail scales. **D.** Longitudinal section of the terminal region of the regenerated tail showing regenerated pad lamellae (arrowheads; for maintaining the orientation with other tail scales, the ventral side is shown upward). **E.** Close-up view of two tail pad lamellae with setae. **F.** Immunolabeled outer and inner setae of a regenerated pad lamella using the core-box antibody for CBPs. Arrows point to the immunofluorescent beta-layer. Dashes underline the epidermis. **G.** Detail of immunolabeled outer setae, especially in the sustaining beta-layer (arrow), using the pre-Core box antibody for CBPs. a, alpha-layer (still forming); ß, beta-layer; ca, regenerated cartilaginous tube; de, dermis; h, hinge region; IS, inner setae; os, outer setae; se, setae; w, wound epidermis. Scale bars: A, C, E, F, 20 μm; B, G, 10 μm; D, 50 μm.

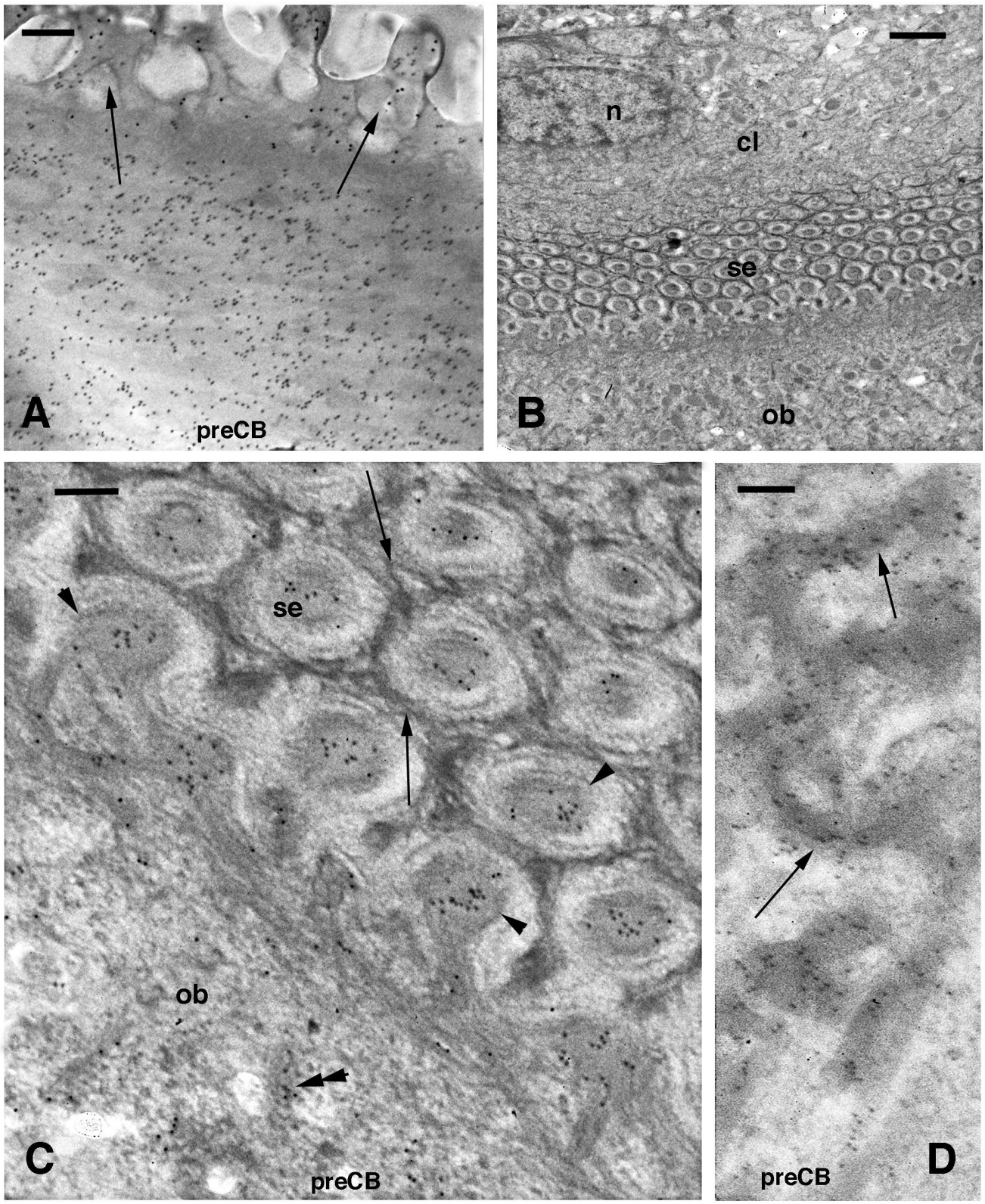

Fig. 5. TEM immunogold (pre-Core Box antibody for CBPs) of the mature and forming setae in *L. capensis*. **A.** Immunolabeled mature beta-layer with the base of setae (arrows). **B.** Formation of the shedding complex area occupied with numerous cross-sectioned setae rows. **C.** Detail on immunolabeled setae formed from the Oberhäutchen layer (arrowheads). The setae are surrounded by a fibrous ring of darker cytoskeletal fibrils (arrows). The double arrowhead indicates a beta-packet. **D.** Details of immunolabeled beta-packets (arrows) present in differentiating beta-cells. cl, clear layer; n, nucleus; ob, Oberhäutchen; se, setae; w, wound epidermis. Scale bars: A, C, D, 0.25 μm; B, 1 μm.

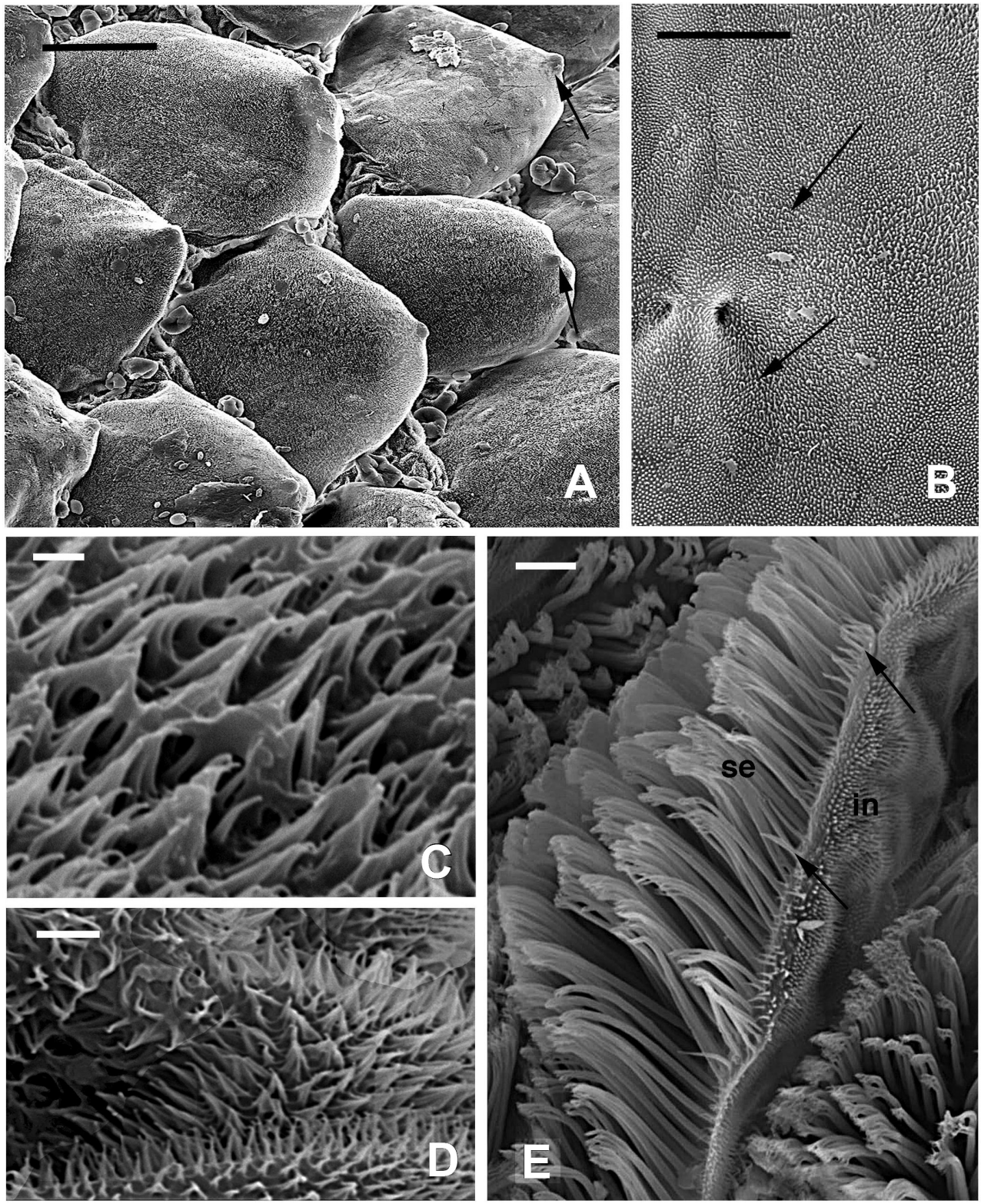

Fig. 6. SEM view of tail scales of *L. conraui* **(A-D)** and tail pad lamella of *L. capensis* **(E)**. **A.** Dorsal tail scales showing the alternated arrangement and the "granulated" surface. Bare spots (arrows) of unknown significance are seen on the caudal tip of the scales. **B.** Higher view showing the apparently fine, granular surface resulting from a carpet of nanoscale dimensional spines. Arrows likely indicate the boundary of Oberhäutchen cells. **C.** Higher view of the spinulated surface. **D.** A higher view of the irregularly oriented and shorter spinulae of the hinge region and inner scale surface. **E.** Pad lamella featuring long setae on the outer surface (se) and shorter filaments (arrows) on the narrow apical border (free margin). The latter continues in the spinulated inner surface of the lamella (in). w, wound epidermis. Scale bars: A, 50 μm; B, 20 μm; C, 1 μm; D, 2 μm; E, 10 μm.

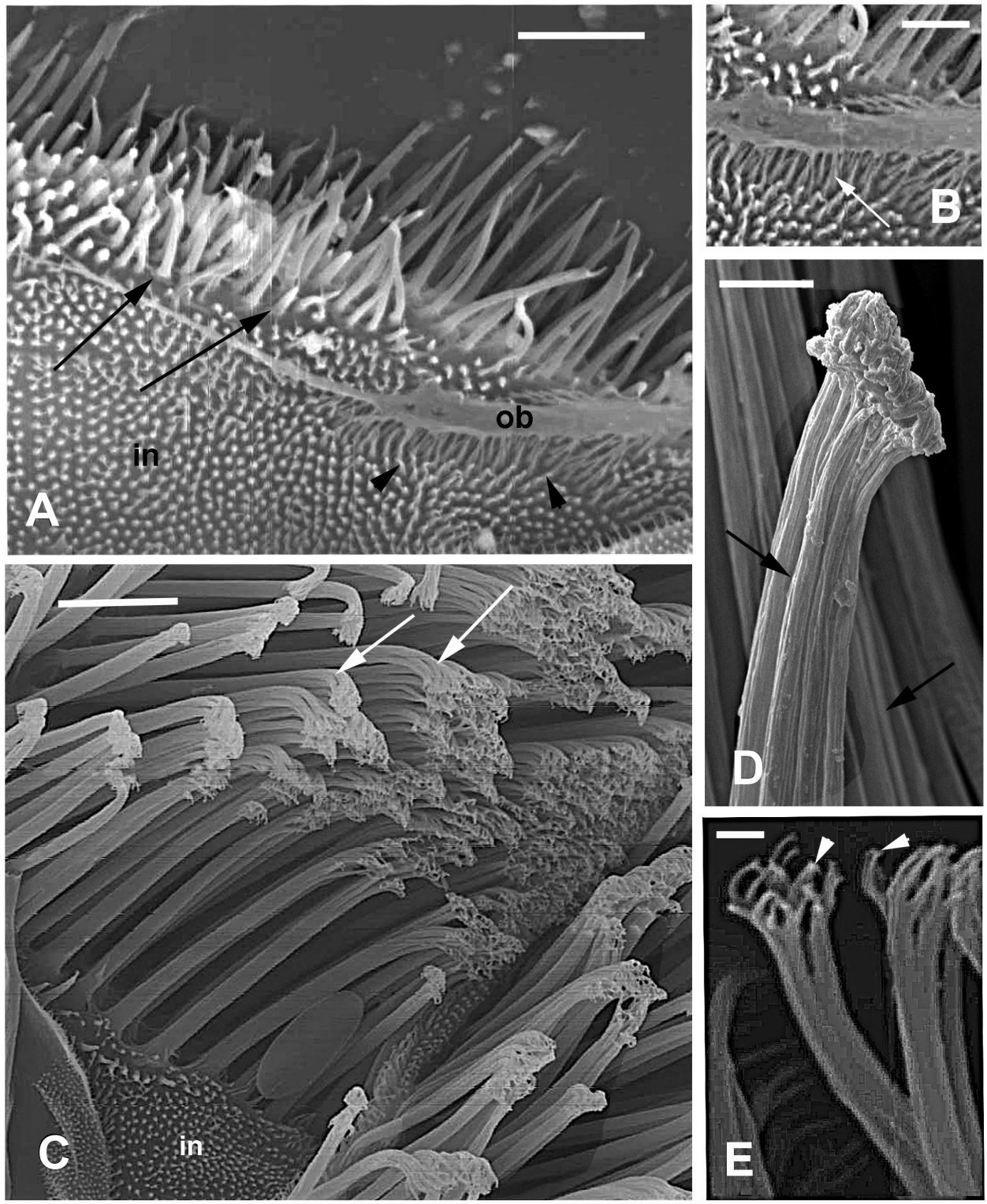

Fig. 7. SEM view of pad lamellae with setae from the normal tail of *L. conraui* **(A, B)** and the regenerating tail of *L. capensis* **(C-E)**. **A.** Detailed view of the apical front of a pad lamella evidencing numerous short filaments (spikes and prongs) of different lengths (arrows) and the even, spinulated carpet present on the inner lamella surface (in). Arrowheads point to a group of thin corneous filaments in continuation with the smooth Oberhäutchen surface (ob). **B.** Detail of the distal margin showing the passage (arrow) from thin corneous filaments into the spinulae of the inner surface. **C.** Small area of a lamella (in indicates a small frame of the inner surface) showing numerous setae with apical curved branching (arrows). **D.** High magnification view of the "condensed" terminal branching of a seta (probably derived from an artifactual stickiness due to the preparation). Arrows indicate the corneous rods forming setae. **E.** Other terminal branching of setae with separated thin branches terminating into spatulae (arrowheads). Scale bars: A, 5 μm; B, 2 μm; C, 10 μm; D, 2 μm; E, 1 μm.

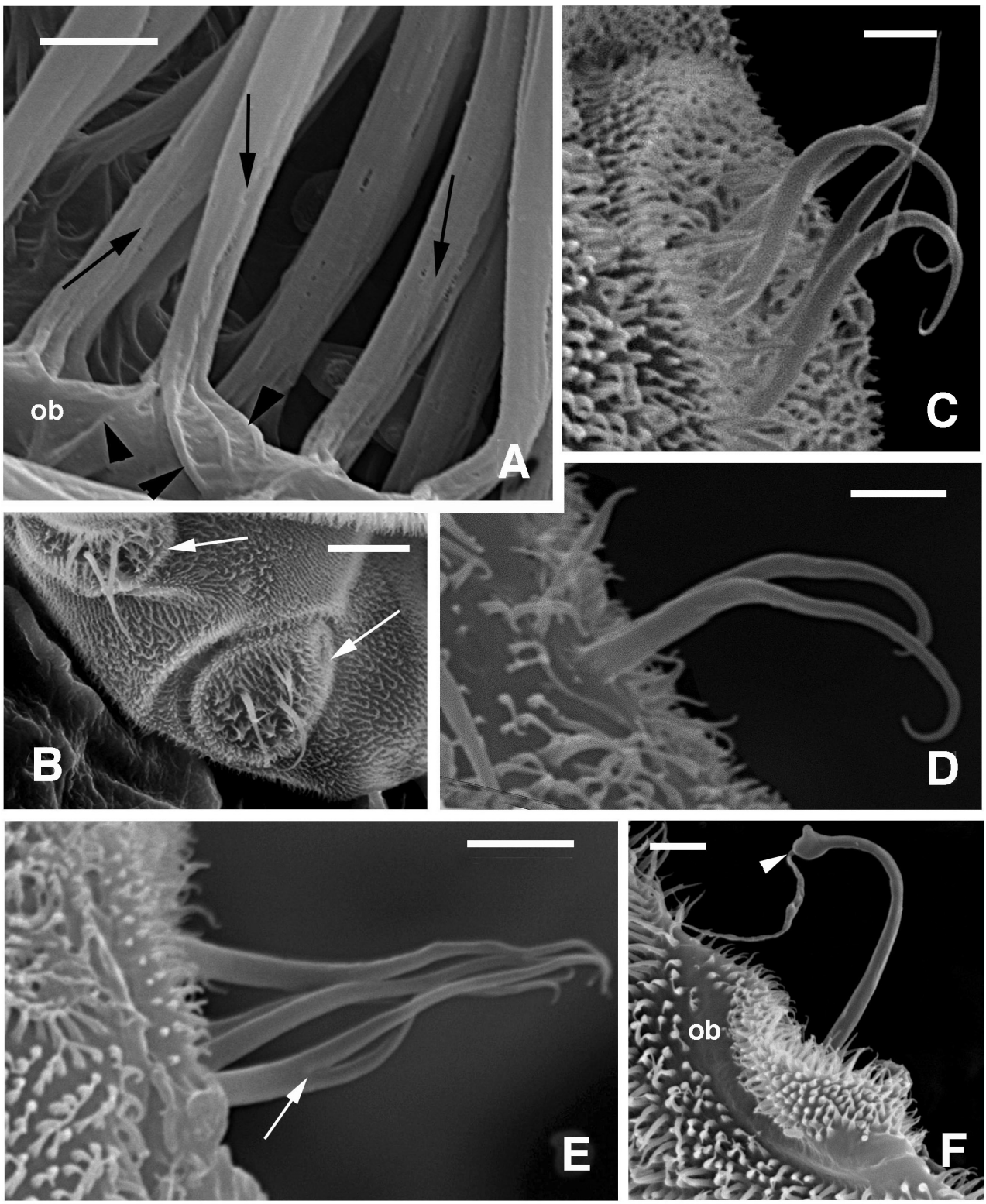

Fig. 8. SEM view of regenerated setae **(A)** and cutaneous sensilli **(B-F)** in the tail of *L. capensis*. **A.** Basal part of setae showing the corneous incisions on the surface (arrows) and the corneous roots (arrowheads) at their base. The latter merge into the cornified Oberhäutchen cell (ob). **B.** Two cutaneous sensilli (arrows) located on the distal border of a tail scale with various corneous (sensorial) filaments. **C.** Detail on the four corneous filaments of a sensillum that tapers in the curved apical part. **D.** Another sensillum with two thinning and curled filaments. **E.** Sensillum showing a branching point (arrow) in one of its corneous filaments. **F.** Sensillum where the single corneous filament forms a terminal knob (arrowhead). The peripheral bed of spinulae is separated from a smooth corneous ring of the Oberhäutchen cell (ob). Scale bars: A, D, F, 2 μm; B, 10 μm; C, E, 2 μm.

length, and formation of corneous Oberhäutchen spines vary along the outer surface of scales, but are shorter in the hinge region and on the inner (ventral) surface of scales, where spines are also less numerous (Fig. 6 C,D, details are reported in Bonfitto et al., 2022).

The surface of pad lamellae forming the scale pads shows a marked difference in length and shape of the microornamentation (Fig. 6E). The outer surface of the lamella (modified outer surface of a scale) in its distal (caudal) part is covered by setae of 1-2 µm in diameter at their base and lengths of 20-30 µm that branch at their tips (Figs. 6E, 7E). The microstructure and terminal branching of tail setae are similar to those of the digits, although their length, 20-30 µm, is generally shorter in tail pads compared with setae present in the digits (Alibardi and Bonfitto, 2019; Bonfitto et al., 2022, 2023a,b). The narrow front side of the lamella (sometimes known as "free margin" in LM or TEM sections) features shorter but variable hairy-like structures of 5-10 µm or longer in length (arrows in Figs. 6E, 7A), but unbranched in their apical part (sometimes known as "spines" and "prongs", Russell and Garner, 2021). Small areas of the free margin appear smooth, but the Oberhäutchen here also forms thin corneous elongations that are in continuation with the spinulae (arrow in Fig. 7B) of the inner surface. This transitional region evidences another variation in the pattern of corneous material deposition on the Oberhäutchen surface. The inner side of the lamella is instead covered by blunt spinulae that form a regular "carpet" (Figs. 6E, 7A). Setae often exhibit a curved shape before branching into 15-30 endings with spatulae of 50-200 nm, the contact area with the substrate (Fig. 7C-E).

Numerous TEM, autoradiographic, *in situ* hybridization, and immunolabeling studies, have indicated that setae derive from the accumulation of packets of corneous material, mainly composed of CBPs, at the base of setae, material that piles up, forming intertwined cords as the main scaffold sustaining the setae (Alibardi, 2018, 2020a,b, 2023; Bonfitto et al., 2022, 2023a,b). Under SEM observation, these cords form shallow incisions or a more irregular

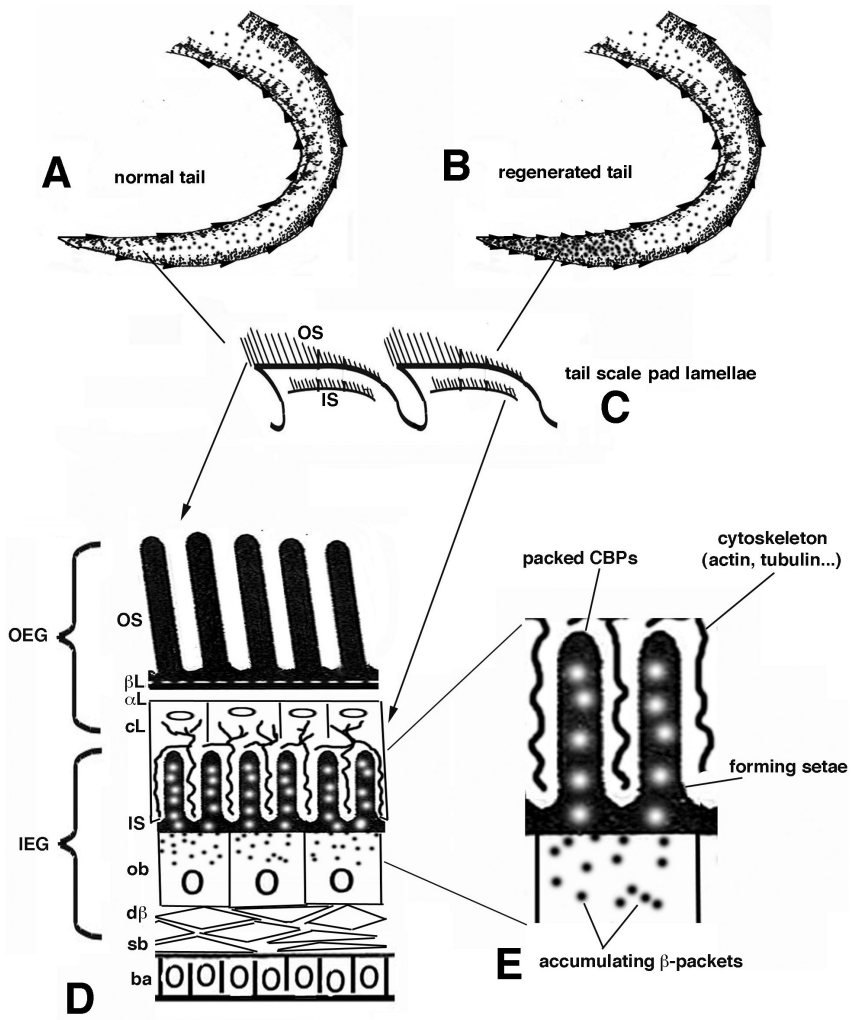

Fig. 9. Schematic drawing illustrating the formation of setae in the tail pads of geckos. At the end of the tail, pads are present in both original (normal **A**) and regenerated **(B)** tails. A section of a tail pad reveals two pad lamellae **(C)** with an outer and inner setal generation (renewal phase). An enlargement of the outer and inner (forming) generations **(D)** is indicated by arrows. In **E**, a cytological detail of inner setal generation is shown, where the Oberhäutchen cytoplasm accumulates beta-packets of CBPs that are packed into the setae surrounded by the cytoplasm of clear cells. αL, alpha-layer; ba, basal layer; ßL, beta layer; CBPs, corneous beta proteins; cL, clear (granulated) layer; dß, differentiating beta-cells; IEG, inner epidermal generation; IS, inner setal generation; ob, Oberhäutchen; OEG, outer epidermal generation; OS, outer setal generation; sb, suprabasal keratinocytes.

striation pattern on the external surface of the setae (arrows in Figs. 7D, 8A). The corneous cords remain as "root-like" cables at the setal base, where they merge with the cornified Oberhäutchen-beta-layer, maintaining the setae tightly attached to pad lamellae (see Fig. 3 in Bonfitto et al., 2022, 2023a,b; Kasper et al., 2024).

Cutaneous sensilli in the tail of some geckoes

The most common cutaneous sensilli, hair-like or setae-bearing, detected in geckos are an elaboration of the spinulated microornamentation pattern of scales (Maderson, 1970; Matveyeva and Ananjeva, 1995; Bauer, 2019; Duisebayeva et al., 2021; Russell and Garner, 2021). They are present in different areas of the body, including the tail, but tend to be more numerous in the head and digital scales (Matveyeva and Ananjeva, 1995; Russell and Garner, 2021). Their number and distribution vary among different gecko species, types of scales, and position on the outer scale surface (Bauer, 1998; Riedel et al, 2019; Riedel and Schwarzkopf, 2022). In the tail of *Lygodactylus*, sensilli are present on the outer surface in some scales and are particularly enriched in digital and tail scales (Griffing et al., 2021; Bonfitto et al., 2022). They are circular, 10-20 µm-long bodies, generally formed by a perimetral "fence" of spinulae surrounding a central area occupied by sparse spinulae and centrally located single or by 3-5 corneous filaments of 0.8-1.2 µm diameter at the base and of variable length, 10-12 µm (Fig. 8B-D). The central sensorial filaments are generally smooth, but in some Australian geckos these filaments form 2-3 branches or even numerous short nano-ramifications, known as "setules" (Riedel et al., 2019; Riedel and Schwarzkopf, 2022). The elongated corneous filaments are often curved at their thin apex (80-120 nm thick), but only in a few cases terminate with a slightly enlarged and flat region of about 500-700 nm that resembles spatulae (Fig. 8C,D).

Sensilli are made from two or a few cells supporting the central one that generates the filaments, and sensilli regenerate during the shedding cycle or after skin loss (Hiller, 1977; Whimster, 1980; Dujsebayeva, 1995). The mechanism of selection of the specific areas where sensilli develop and their differentiation remains unknown, but they are always associated with a localized innervation (Hiller, 1976, 1977; von During and Miller, 1979; Whimster, 1980; Dujsebayeva, 1995). A histological and ultrastructural study revealed that the filament of the sensilli is formed in contact with a granulated or clear layer, resembling the process of digital setae formation (Hiller, 1977; Dujsebayeva, 1995). Aside from a mechanical receptor role, they may serve other functions, including thermal or hydrophilic sensation, namely environmental humidity (Matveyeva and Ananjeva, 1995; Riedel et al., 2019; Riedel and Schwarzkopf, 2022).

In conclusion, in the Gekkonidae family, a basic spinulated microornamentation pattern is elaborated into multiple variations that produce spinules, spikes, prongs, variably long setae, and sensorial setae, the latter associated with nerve endings. All these micro-ornamentations, and in particular the setae, derive from the differentiation of two interfaced layers of the gecko epidermis, the clear layer of the outer epidermal generation with the Oberhäutchen layer of the inner epidermal generation (Fig. 9). While spinulated microornamentation forms mainly a protective surface, the elaboration of prongs and setae has assumed new functions during gecko evolution: adhesion (setae) and sensorial (sensilli). Therefore, although not soft and pliable like the mammalian skin surface, the skin of geckos, and more generally of reptiles, is equipped with a complex and multi-variant sensorial apparatus that endows them with broad sensorial capability.

Acknowledgements. the study was self-funded by Comparative History Lab, Padova, Italy and also financed from the Canziani Bequest Fund (AB; grant number A31. CANZELSEW, University of Bologna). The authors thank Dr. Roberta Randi (University of Bologna) for her assistance with SEM observations.

References

Alibardi L. (1999). Keratohyalin-like granules in embryonic and regenerating epidermis of lizards and *Sphenodon punctatus* (Reptilia, Lepidosauria). Amphibia-Reptilia 20, 11-23.

Alibardi L. (2014). Immunolocalization of alpha-keratins and associated beta-proteins in lizard epidermis shows that acidic keratins mix with basic keratin-associated beta-proteins. Protoplasma 251, 827-837.

Alibardi L. (2018). Review: Mapping proteins localized in adhesive setae of the Tokay gecko and their possible influence on the mechanism of adhesion. Protoplasma 255, 1785-1797.

Alibardi L. (2020a). Adhesive pads of geckos and anoline lizards utilize corneous and cytoskeletal proteins for setae development and renewal. J. Exp. Zool. B Mol. Dev. Evol. 334, 263-279.

Alibardi L. (2020b). Immunolocalization of corneous proteins including a serine-tyrosine-rich beta-protein in the adhesive pads in the tokay gecko. Microsc. Res. Tech. 83, 889-900.

Alibardi L. (2023). The periodic replacement of adhesive setae in pad lamellae of climbing lizards is driven by patterns of corneous layer growth. J. Dev. Biol. 11, 3

Alibardi L. and Bonfitto A. (2019). Morphology of setae in regenerating caudal adhesive pads of the gecko *Lygodactylus capensis* (Smith, 1849). Zoology 133, 1-9.

Alibardi L. and Meyer-Rochow BM. (2017). Regeneration of tail adhesive pad scales in the New Zealand gecko *Hoplodactylus maculatus* (Reptilia; Squamata; Lacertilia) can serve as an experimental model to analyze setal formation in lizards generally. Zool. Res. 38, 1-11.

Arnold E.N. (2002). History and function of scale microornamentation in lacertid lizards. J. Morphol. 252, 145-169.

Bauer A.M. (1998). Morphology of the adhesive tail tips of *Carphodactyline geckos* (Reptilia: Diplodactylidae). J. Morphol. 235, 41-58.

Bauer A.M. (2019). Gecko adhesion in space and time: A phylogenetic perspective on the scansorial story. Comp. Int. Biol. 59, 117-130.

Bonfitto A., Bussinello D. and Alibardi L. (2022). Electron microscopic analysis in the gecko *Lygodactylus* reveals variations in micro-ornamentation and sensory organs distribution in the epidermis that indicates regional functions. Anat. Rec. 306, 1990-2014.

Bonfitto A., Randi R. and Alibardi L. (2023a). Bristle formation in adhesive pads and sensilli of the gecko *Tarentola mauritanica* derive from a massive accumulation of corneous material in Oberhautchen cells of the epidermis. Micron 171, 103483.

Bonfitto A., Randi R., Magnani M. and Alibardi L. (2023b). Micro-ornamentation patterns in different areas of the epidermis in the gecko *Tarentola mauritanica* reflect variations in the accumulation of corneous material in Oberhautchen cells. Protoplasma 260, 1407-1420.

Collins C.E., Russel A.P. and Higham T.E. (2015). Subdigital adhesive pad morphology varies in relation to structural habitat use in the Namib day gecko. Funct. Ecol. 29, 66-77.

Dujsebayeva T.N. (1995). The microanatomy of regenerated bristle receptors of two gecko species, *Cyrtopodion fedtschenkoi* and *Sphaerodactylus roosevelti*. Russ. J. Herpethol. 2, 58-64.

Dujsebayeva T., Ananieva N. and Bauer A.M. (2021). Scale microstructure of pygopodid lizards (Gekkota: Pygopodidae). Phylogenetic stability and ecological plasticity. Russ. J. Herpethol. 28, 291-308.

Gamble T., Greenbaum E., Jackman T.R., Russell A.P. and Bauer A.M. (2012). Repeated origin and loss of adhesive toepads in geckos. PLoS One 7, e39429.

Griffing A.H., Sanger T.J., Epperlein L., Bauer A.M., Cobos A., Higham T.E., Naylor E. and Gamble T. (2021). And thereby hangs a tail: morphology, developmental patterns and biomechanics of the adhesive tail of crested geckos (*Correlophus ciliatus*). Proc. Royal Soc. B 288, 20210650.

Griffing A.H., Gamble T., Cohn M.J. and Sanger T.J. (2022). Convergent developmental patterns underlie the repeated evolution of adhesive to pads among lizards. Biol. J. Linnean Soc. 135, 518-532.

Hiller U. (1972). Licht- und elektronenmikroskopische untersuchungen zur haftborstenentwicklung bei *Tarentola mauritanica* L. (Reptilia, Gekkonidae). Zeitfr. Morphol. Tiere 73, 263-278.

Hiller U. (1975). Comparative study on the functional morphology of two gekkonid lizards. J. Bombay Natural History Soc. 73, 278-282.

Hiller U. (1976). Elektronenmikroskopische Untersuchungen zur funktionellen Morphologie der borstenführenden Hautsinnesorgane bei *Tarentola mauritanica* L. (Reptilia, Gekkonidae). Zoomorphologie 84, 211-221.

Hiller U. (1977). Regeneration and degeneration of setae-bearing sensilla in the scales of the gekkonid lizard *Tarentola mauritanica* L. Zool. Anz. 199, 113-120.

Irish F.J., Williams E.E. and Seiling E. (1988). Scanning electron microscopy of changes in epidermal structure occurring during the shedding cycle in squamate reptiles. J. Morphol. 197, 105-126.

Kasper J.Y., Laschke M.W., Koch M., Alibardi L., Magin T., Niessen C.M. and del Campo A. (2024). Actin-templated structures: nature's way to hierarchical surface patterns (Gecko's setae as case study). Adv. Sci. 11, 2303816.

Maderson P.F.A. (1970). Lizard glands and lizard hands: models for evolutionary study. Forma Functio 3, 179-204.

Maderson P.F.A. (1971). The regeneration of caudal epidermal specializations in *Lygodactylus picturatus keniens*is (Gekkonidae, Lacertilia). J. Morph. 134, 467-478.

Maderson P.F.A., Rabinowitz T., Tandler B. and Alibardi L. (1998). Ultrastructural contributions to an understanding of the cellular mechanisms involved in lizard skin shedding with comments on the function and evolution of a unique lepidosaurian phenomenon. J. Morphol. 236, 1-24.

Matveyeva T.N. and Ananjeva N.B. (1995). The distribution and number of the skin sense organs of agamids, iguanid and gekkonid lizards. J. Zool. 235, 253-268.

McCann J. and Hagey T.J. (2024). Early burst of parallel evolution describes the diversification of toe pads. Front. Ecol. Evol. 11, 1334870.

Niewiarowski P.H., Stark A.Y. and Dhinojwala A. (2016). Sticking to the story: Outstanding challenges in gecko-inspired adhesives. J. Exp. Biol. 219, 912-919.

Riedel J. and Schwarzkopf L. (2022). Variation in density, but not morphology, of cutaneous sensilla among body regions in nine species of Australian geckos. J. Morphol. 283, 637-652.

Riedel J., Vucko M.J., Blomberg S.P., Robson S.K. and Schwarzkopf L. (2019). Ecological association among epidermal microstructure and scale characteristics of Australian geckos (Squamata: Carphodactylidae and Diplodactylidae). J. Anat. 234, 853-874.

Ruibal R. (1968). The ultrastructure of the surface of lizard scales. Copeia 4, 698-703.

Russell A.P. and Gamble T. (2019). Evolution of the gekkotan adhesive system: does digit anatomy point to one or more origin? Int. Comp. Biol. 59, 131-147.

Russell A.P. and Garner AM. (2021). Setal field transects, evolutionary transitions and gecko-Anole convergence provide insights into the fundamentals of form and function of the digital adhesive system of lizards. Front. Mechan. Engineer. 6, 621741.

Russell A.P, Stark A.Y. and Higham T.E. (2019). The integrative biology of gecko adhesion: Historical review, current understanding and grand challenges. Integr. Comp. Biol. 59, 101-116.

von Düring M. and Miller R. (1979). Sensory nerve endings in the skin and deeper structures. In: Biology of the Reptilia. Vol. 9. Neurology A. Gans C. Northcutt R.G. and Ulinski P (eds). Academic Press, New York. pp 407-442

Whimster I.W. (1980). Neural induction of epidermal sensory organs in gecko skin. In: The skin of vertebrates. Spearman R.I.C. and Riley P.A. (eds). Linnean Soc. Symposium n. 9. Academic Press, London. pp 161-167.

Accepted September 8, 2025